

Sustained growth of nanotubes by self-assembly of DNA strands at room temperature

Laura Bourdon,^{1,†} Syed Pavel Afrose,^{2,†} Siddharth Agarwal,² Aurélie Di Cicco,³ Daniel Lévy,³ Ayako Yamada,¹ Damien Baigl,^{1,*} Elisa Franco^{2,*}

¹PASTEUR, Department of Chemistry, École Normale Supérieure, PSL University, Sorbonne Université, CNRS, 75005 Paris, France

²Department of Mechanical and Aerospace Engineering, University of California at Los Angeles, 420 Westwood Plaza, Los Angeles, CA 90024

³Institut Curie, Université PSL, Sorbonne Université, CNRS UMR168, Laboratoire Physico-Chimie Curie, 75005, Paris, France

[†]These authors contributed equally

*Corresponding authors: damien.baigl@ens.psl.eu, efranco@seas.ucla.edu

Abstract

Artificial biomolecular nanotubes are a promising approach to build materials mimicking the capacity of the cellular cytoskeleton to grow and self-organize dynamically. Nucleic acid nanotechnology has demonstrated a variety of self-assembling nanotubes with programmable, robust features, and morphological similarities to actual cytoskeleton components. However their production typically requires thermal annealing that is not only incompatible with physiological conditions but also hinders the possibility for continuous growth and dynamic self-organization. Here we report DNA nanotubes that self-assemble from a simple mixture of five short DNA strands at constant room temperature, with remarkable capability to sustainably grow over prolonged time. The assembly, done in a monovalent salt buffer (here, 100 mM NaCl), ensures that the nanoscale features of the nanotubes are preserved under these isothermal conditions, enabling continuous growth up to 20 days and the formation of individual nanotubes with near flawless arrangement, a diameter of 22 ± 4 nm, and length of several tens of micrometers. We demonstrate the crucial role of the monovalent cation to achieve such properties. We finally encapsulate the strands in micro-sized compartments, such as water-in-oil microdroplets and giant unilamellar vesicles serving as simple cell models. Notably, nanotubes not only isothermally grow in these conditions, but also self-organize into dynamic higher-order structures, such as rings and dynamic networks, demonstrating that cytoskeleton-like properties can emerge from a combination of sustained growth and confinement. Our study suggests a method for engineering biomolecular scaffolds and materials that display sustained dynamic and life-like properties.

Introduction

Through billions of years of evolution, Nature came up with complex self-assembled architectures capable of performing functions crucial for biological machinery to operate seamlessly. These self-assembled structures are highly dynamic and possess the capability to grow, adapt and reconfigure. For example, the cytoskeleton protein filaments are highly dynamic non-equilibrium self-assemblies that show remarkable spatiotemporal control over functions that regulate cell life-cycle, motility and so forth.^[1,2] Creating synthetic self-assembled architectures that can demonstrate such dynamic and adaptive behavior can lead to materials with precise control over properties with potential application in diverse fields, from drug delivery to sensing.^[3] Nucleic acid (NA) nanotechnology is a powerful tool in this regard as it offers great programmability and versatility through simple modification of strand sequences.^[4] By rationally designing the NA sequences according to Watson-Crick-Franklin base-pairing rules, parts of the different strands can be made

complementary to each other, which can then hybridize to give rise to desired morphologies.^[5,6] Using the assembly of DNA tiles interacting through their sticky ends, self-assembled nanotubes have been produced^[7-9] which resemble the cytoskeleton and actin filaments from a structural viewpoint.^[9-14]

Although reconfigurability of DNA nanostructures is possible by using strategies such as strand displacement,^[15] electrostatic suprafolding^[16] and photocontrol,^[8,17-19] building structures capable of spontaneous growth and morphological adaptation is challenging yet highly desirable. In fact, most DNA nanostructures produced to date have a definite size and shape with limitations in both space and time. In the case of DNA origami, for instance, the limitation in space is mainly due to the use of a scaffold that restricts the size of the final objects to around or below 100 nm.^[5,20] Several alternatives to this approach have been proposed, from scaffold-free self-assembly protocols^[21] to self-assembly of pre-formed origamis.^[22-25] However, in most of these cases, the formation of the targeted assembly has required the use of a thermal annealing step where the initial mixture containing the DNA strands is heated above the DNA melting temperature prior to a slow cooling down process. This creates a strong temporal constraint as the resulting nanostructures are thermodynamically stable and usually do not display dynamic behavior or evolve anymore in shape and size over time.

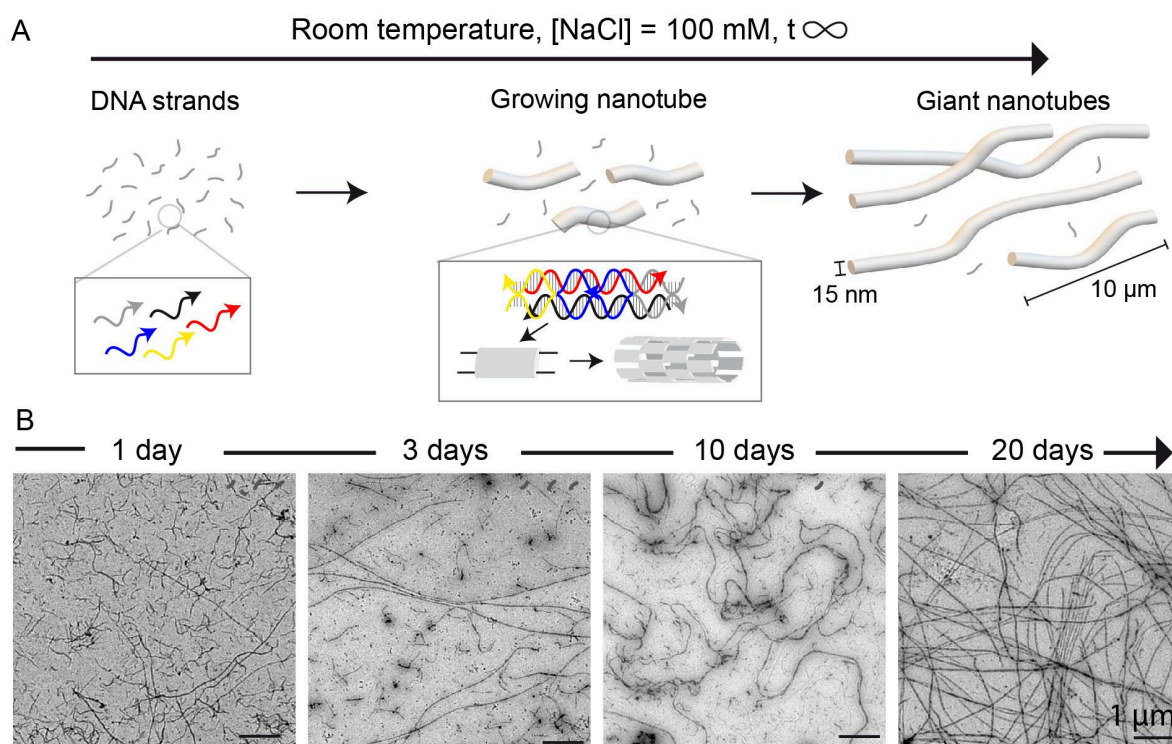


Figure 1. Formation of micrometer-long DNA nanotubes at constant room temperature. A) A mixture of five DNA strands in TANa buffer (Trizma base 40 mM, acetic acid 20 mM, 100 mM NaCl) self-assemble isothermally into a self-repeating tile motif forming nanotubes which grow in solution at room temperature over a prolonged period of time. B) Representative transmission electron microscopy (TEM) images of nanotubes obtained after 1, 3, 10 and 20 days of self-assembly at room temperature in TANa. Each strand concentration was 500 nM.

Isothermal assembly is an interesting alternative to achieve dynamic structures because, by fixing the temperature, structures can be intrinsically more reconfigurable and free to evolve, and potentially grow, without any time constraints. It was shown, for instance, that using a simple buffer composed of NaCl, complex cocktails of DNA strands could self-assemble at room temperature into elaborate nanostructures, which not only reproduced the desired DNA-encoded morphology but were also highly reconfigurable and capable of shape

selection, optimisation and transformation.^[26] This approach was applied to the isothermal self-assembly of DNA origamis and single-stranded tiles, leading to two- or three-dimensional objects no larger than 100 nm. Using strands coding for self-repeating units, nanogrids were produced but defect-free assembly of a maximum of a few hundred of nm were observed.^[26] To explore the possibility of building longer-growing nanostructures that could approach cytoskeleton dimensions and dynamic organization, we selected a system consisting of merely five oligonucleotides forming a double-crossover tile that further assembles into cylindrical nanostructures called nanotubes.^[7] This design has been studied for many years, including for constructing biomimetic endo- or exo-cytoskeletons,^[10,11,14] but nanotubes were always obtained either by thermal annealing or by the self-assembly of pre-annealed tiles, limiting possibilities of growth and evolution at fixed temperature. In this work, the oligonucleotides are mixed in an NaCl buffer and we study their evolution over time at room temperature, without any thermal pre- or post-treatment (Figure 1A). Notably, we observe the autonomous formation of nanotubes growing into very large dimensions and self-organizing into dynamic networks when confined in biomimetic compartments. Using fluorescence, transmission electron and cryo-electron microscopy, we characterize the dynamic and structural features of these live-growing structures in bulk, in droplets and in giant liposomes.

Results

We chose DNA nanotubes assembling from double-crossover (DX) tiles^[7] requiring the presence of only five short, distinct DNA strands designed to interact as depicted in Figure 1A *left*. These strands form two DNA double helices held together as three of the strands (yellow, blue, and gray in Figure 1A) cross over from one helix to the other, forming two junctions that confer rigidity to the tile. The 5'-end of the strand in the center of the tile (blue in Figure 1A) was modified with the Cy3 dye to enable fluorescence microscopy observation. Tiles interact via complementary single stranded domains known as sticky ends (at the 5' and 3' end of the yellow and gray strands). The inter-tile crossover distance is chosen so that individual tiles bind to each other at an angle, and thus form micrometer-scale tubular structures rather than flat lattices^[7,27,28]. Because these DNA nanotubes can be engineered to work as scaffolds with the capacity to respond to biochemical and physical stimuli, they are excellent components to build an “artificial cytoskeleton” for synthetic cells and responsive biomaterials^[9,10,14]. A notable limitation toward this has been the requirement to thermally anneal the DX tiles^[7,27–29], which is at odds with the goal of building life-like systems operating at constant temperature. With the objective to build nanostructures that can grow under life-compatible conditions, we placed the DNA strands in a buffer exclusively composed of monovalent cations, dubbed “TANa” buffer (Trizma base 40 mM, acetic acid 20 mM, 100 mM NaCl), which was recently shown to enable successful assembly of complex DNA nanostructures at constant room temperature.^[26] Doing so, we questioned not only whether DNA nanotubes could assemble isothermally at room temperature but also how they would self-organize over time (Figure 1A *middle, right*). To evaluate the performance and understand the advantage of using monovalent salts, we compared the results to those obtained with the magnesium-containing buffers conventionally used for DNA self-assembly, either TAMg (Trizma base 40 mM, acetic acid 20 mM, 12.5 mM MgCl₂) or TAEMg (TAMg + 1 mM EDTA).

Incubation of the five tile-forming DNA strands in TANa buffer readily produced DNA nanotubes, which grew in solution for days at room temperature as observed by fluorescence microscopy (Movie S1). Transmission electron microscopy (TEM) qualitatively shows that short nanotubes slowly disappear while longer ones become predominant (Figure 1B). After 20 days, very long nanotubes (>10 μm) dominate in the sample, with a vanishing number of shorter tubes (1-2 μm), signifying the ongoing growth of the nanotubes over a long period of time. To analyze the effect of ions on nanotubes stability, we used fluorescence microscopy image analysis to estimate the nanotube melting temperature (T_m).

We found that nanotubes formed by isothermal assembly in TANA have a lower T_m ($\sim 32^\circ\text{C}$) when compared to those obtained by thermal annealing in TAEMg buffer ($T_m \sim 38^\circ\text{C}$), as discussed in the Supplementary Information (SI) Section 4.

TEM images at higher magnification in Figures 2A, *top* confirm that isothermal assembly in TANA enables enough reconfigurability for the formation of distinct individual nanotubes while allowing their continuous growth over time up to micrometer length. When the same isothermal formation experiment was done in TAMg buffer, replacing NaCl with 12.5 mM MgCl_2 , nanotubes could still be detected in TEM images but were highly clustered in the form of micrometer-sized aggregates (Figure 2A, *bottom*, Movie S2) that can be attributed to a stronger stabilization of the DNA nanostructures by divalent Mg^{2+} cations.

Cryo-electron microscopy revealed a highly regular internal structure of the nanotubes with well-defined tiles aligned with the principal axis of the nanotubes (Figure 2B), confirming that the circumference of a nanotube generally includes 6-7 tiles, an internal structure comparable to that obtained by thermal annealing in the presence of magnesium (Figure S1).^[7] However, we noted that the diameter obtained by isothermal assembly in TANA (22 ± 4 nm, Figure S2A) was shifted to higher values compared to the one obtained by thermal annealing in TAMg (12 ± 2 nm, Figure S2B) probably due to higher flexibility provided by the monovalent salt conditions. Isothermal assembly thus allowed both faithful assembly of DNA strands and sustained growth into soft and well-defined individual DNA nanotubes.

To get insights into the dynamics underlying the first hours of isothermal self-assembly, we used fluorescence microscopy and automated image analysis to establish the length distribution of nanotubes adsorbed on glass slides at different assembly times (Figure 3). In TANA buffer (Figure 3A), the average nanotube length progressively increased with time, reaching up to 5.7 ± 0.35 μm at 24 h (Figure 3B, S3) accompanied by a progressive shift of the distribution (Fig 3C top). To get a clearer picture of how monomers are distributed in the tubes, we also plotted the fraction of the total measured nanotube length occupied by each size range (Figure 3C bottom). These length fraction plots show that the contribution of short nanotubes diminishes over time, as longer ones dominate, consistent with what we observed on a longer time scale by TEM (Figure 1B). To better understand the specificity of NaCl for isothermal growth, we set-up a protocol allowing isothermal assembly in the presence of Mg^{2+} . Four tile strands were first thermally annealed in TAEMg, prior to introduction of the fifth strand (gray strand in Figure 1A, time zero) and isothermal assembly at room temperature (Figure 3D). Representative microscopy images show the growth of the tubes over time (Figure 3E, S3). The average length of nanotubes in TAEMg plateaus after around 30 minutes, in striking contrast to the growth in TANA buffer. The early saturation was also evident from both the frequency-based and length fraction histograms (Figure 3F).

To gain more insights on the growth mechanisms in TANA buffer when compared to TAEMg buffer, we plotted the cumulative complementary distribution function (CCDF) of the nanotube length in each case (Figure 3G-J). These CCDF plots estimate the likelihood to find a nanotube larger than a given value. DNA nanotube length is expected to follow an exponential distribution^[27], whose CCDF is a straight line in a semilogarithmic plot, as confirmed in Figures 3G and I. When normalized with respect to its average, any exponential CCDF should collapse on a straight line with slope -1 ^[30]. While data for both TANA and TAEMg incubated nanotubes generally follow this trend (Figure 3H, J), we note significant discrepancy with respect to the exponential model for TANA incubated nanotubes. In particular, during the initial phases of growth the system is less likely to present long nanotubes when compared to the exponential case, while at later phases it is more likely to produce long nanotubes. A possible explanation for this behavior is that TANA-assembled tiles may be initially less abundant, hindering polymerization; alternatively, nucleation events may be very frequent in TANA conditions due to the more dynamic interactions among DNA strands, which would result in a larger number of shorter nanotubes. At a longer timescale, we hypothesize that again the enhanced capacity of tiles to dynamically interact in TANA may promote end-joining of existing nanotubes, resulting in overall longer assemblies.

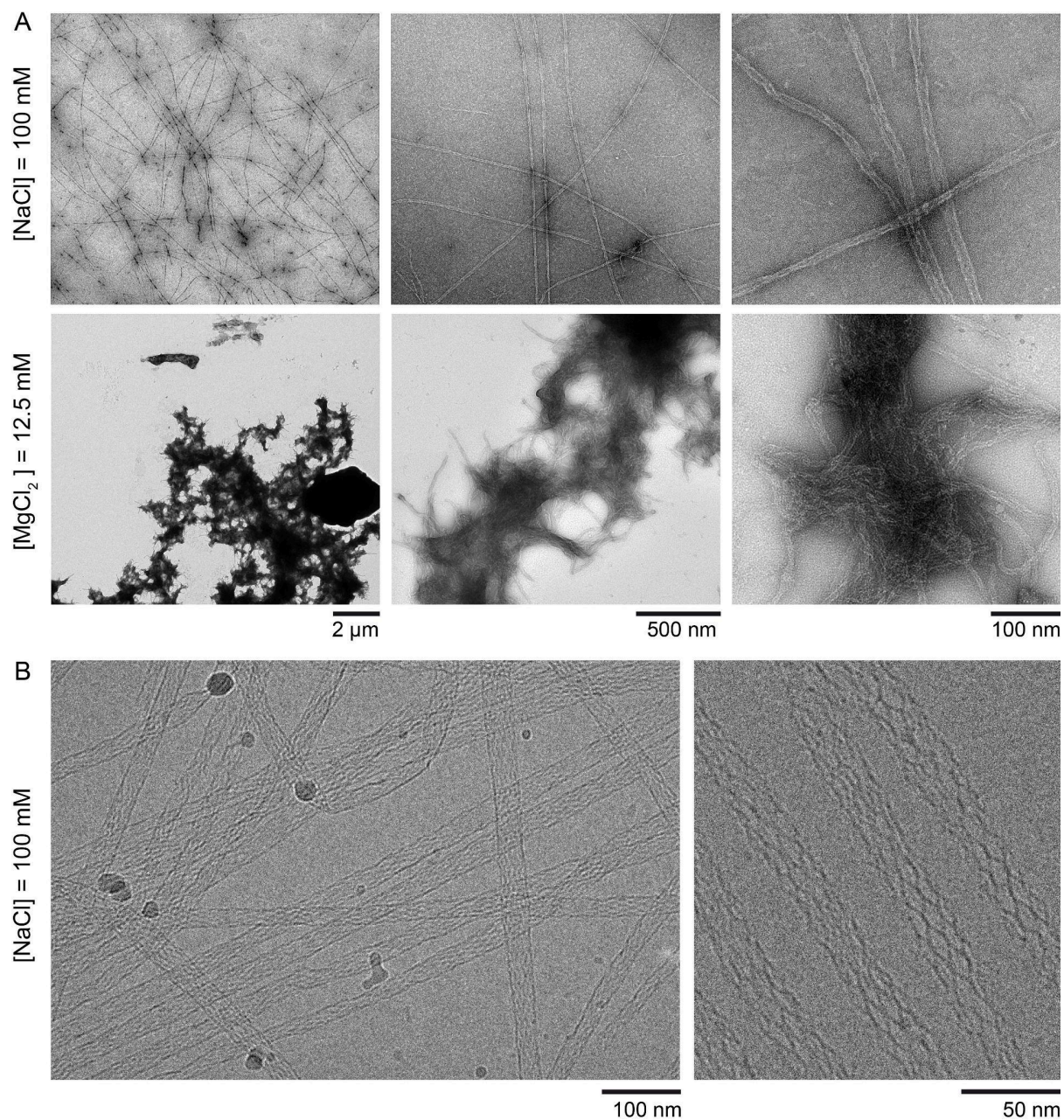


Figure 2. NaCl allows the isothermal assembly of individual, well-defined nanotubes at room temperature. A) TEM images of DNA nanotube self-assembly at room temperature for 20 days in a TA buffered solution containing either 100 mM NaCl (TANa, top) or 12.5 mM $MgCl_2$ (TAMg, bottom), at three magnifications. Each DNA strand was 500 nM. B) Cryo-electron microscopy images of DNA nanotubes obtained by isothermal assembly at room temperature in TANa. Each DNA strand was 500 nM with assembly times of 10 days (left) and 5 h (bottom right)

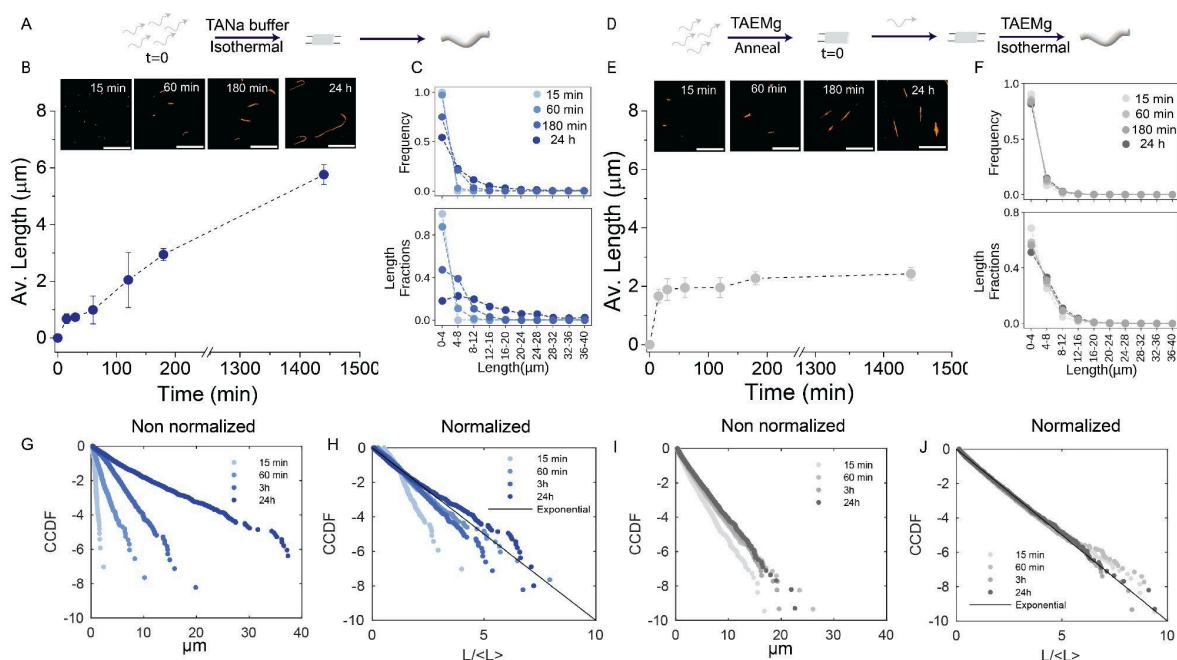


Figure 3. Growth of DNA nanotubes made from single-tile designs in TANA and TAEMg buffers. (A) Scheme showing the isothermal assembly process in TANA buffer, (B) microscopy images and average nanotube length at different time points, and (C) frequency and length fraction histograms. (D) Scheme showing the isothermal assembly process of nanotubes in TAEMg buffer; (E) microscopy images and average nanotube length at different time points, (F) frequency and length fraction histograms. (G-J) Normalized and non-normalized CCDF plots of nanotube length for samples in TANA (G, H) and in TAEMg (I, J). The concentration of each strand in these experiments is 1 μM . Scale bars= 10 μm . Error bars represent the standard deviation of the mean over 3 experimental replicates.

We then verified that a different nanotube variant, including two distinct tiles (a total of ten DNA strands), assembles correctly in TANA buffer (Figure S4,S5). These tiles (dubbed SEp and REp by Rothmund^[7]) have mutually complementary sticky ends that result in the assembly of nanotubes with parallel “rings” of distinct tiles (Figure S4).^[9] Surprisingly, the average length of these nanotubes does not increase as much as in the single tile case, although trends for the length histograms, length fractions, and CCDF plots are consistent with the single tile case when compared with tiles annealed in TAEMg (Figure S6-S11). We hypothesize that the lack of sustained growth may be due to a loss of end-joining capability introduced by “irregular” growth edges when the parallel rings are incomplete. Interestingly, the TANA buffer allows the growth of the nanotubes with or without prior incubation of the strands to form the tiles (Figure S4, S5, S9-S11).

Overall, we demonstrated that the TANA isothermal conditions allow a simple mix of five DNA strands to self-assemble into nanotubes that grow over days, exceeding the average length achievable with the conventional TAEMg assembly buffer. Given the growing interest in using DNA scaffolds toward the development of composite biomaterials and synthetic cells, we then studied how TANA-assembled nanotubes self-organize when confined in micro-compartments, starting with water-in-oil (W/O) emulsion droplets made of a fluorinated oil and biocompatible-surfactant mixture (Figure 4A)^[9,31]. The five strands of the single tile design (100 nM in TANA) were encapsulated inside the droplets and the system was incubated at room temperature. With time, the tubes were formed and grew inside the droplets. Notably, after a day, the nanotubes formed started to reorganize inside the droplets to create branched networks (Figure 4B), in contrast with the bulk conditions where only longitudinal structures were detected. (Figure 1B, 2). After two days, dense networks were observed inside the droplets, suggesting continued nanotube growth as tiles polymerize. Growth in confinement also induced the formation of bent structures and ring-like

morphologies (Figure 4C). Further, example time-lapse microscopy images and supplementary videos (Figure S12, Movie S4) show the mobile nature of the nanotubes inside the droplets.

Next, we asked if isothermal assembly can be extended to compartments that have a membrane, using Giant Unilamellar Vesicles (GUVs) as closer mimics of synthetic cellular micro-environments. GUVs were prepared by adapting emulsion transfer protocols (Figure 4D, Supplementary Information for details).^[32–34] Contrary to previous works,^[10,14] we did not encapsulate preformed tiles or nanotubes, but directly the five strands (1-5, 500 nM each in TANA) in the GUVs, and let the system evolve over time. Encapsulation of the DNA strands within the lipid membrane was successful as indicated by the observation of fluorescence (Cy3-labeled strand 3) in the vesicle interior (Figure 4E) and its membrane (Figure S13). We subsequently monitored the isothermal growth and reorganization of nanotubes inside the liposomes. After 2 days, individual nanotubes could be observed inside the vesicles, showing that isothermal growth was also occurring in these cell-like microenvironments. From day 4, nanotubes self-organized into dynamic higher-order structures, such as networks and ring-like morphologies (Figures 4E, 4F, Movie S3), recapitulating the behavior observed in microdroplets. Interestingly, similar reorganization of DNA nanotubes into cytoskeleton-like assemblies inside GUVs has been recently reported, but it always involves the addition of condensing agents, such as crowding agents or high concentration of Mg^{2+} .^[10,14] Here we find that the combination of isothermal self-assembly from molecular bricks (DNA strands) with confinement is enough to generate such highly-dynamic self-organization, in a way probably close to how living systems actually work. Overall, the isothermal growth of DNA nanotubes inside W/O droplets and vesicles suggest that they are a viable approach to build dynamic, responsive scaffolds in synthetic cells and living materials. Isothermally assembling DNA nanotubes can form adaptive architectures that may be engineered to achieve spatiotemporal control over compartment functions and mimic the dynamic and highly reconfigurable nature of cytoskeleton components.

Discussion and conclusions

We demonstrated the isothermal growth of DNA nanotubes at room temperature using a Mg-free monovalent NaCl containing buffer (TANA) without the need of an annealing step. Starting from a mixture of 5 different DNA strands, nanotubes with the desired structure grow for days as verified through different microscopic techniques such as TEM, cryo-electron microscopy and fluorescence microscopy. Frequency and length fraction analysis show the gradual disappearance of smaller nanotubes and appearance of longer nanotubes over time, likely because joining events are more favorable when compared to the case of assembly using divalent cations that favor kinetic trapping. This results in a sustained growth over days allowing a simple molecular program of a few elementary self-assembling bricks to reach mesoscopic dimensions (1 - 100 μm) while ensuring near flawless assembly at the nanoscale level. This characteristic constitutes a promising asset for the design of future self-assembled smart materials capable of adaptation and self-healing.

The NaCl-based buffer allowed the nanotubes to self-assemble isothermally inside compartments (water-in-oil droplets as well as giant unilamellar vesicles serving as cell models), where they not only grow but also spontaneously reorganize, without addition of any crosslinking or condensing agents, into dynamic higher-order assemblies such as networks and ring-like structures, forming a valuable example of confinement-induced self-organization in a synthetic cell-mimicking system.

We found that the use of TANA buffer caused a decrease in the nanotube melting temperature relative to when they were grown in TAEMg. This suggests a lower thermodynamic stability of the nanotubes formed in TANA buffer: this is an advantage in terms of dynamic reconfigurability of the structures, but could pose a challenge for growing nanotubes at physiological temperatures in biological applications^[35]. However, stability could be easily improved by increasing the length of the tile sticky ends. Another approach could

be to optimize the buffer composition to include limited amounts of $MgCl_2$ to enhance thermal stability. Inclusion of $MgCl_2$ is often also required for proper enzyme activity, for example in the case of *in vitro* RNA transcription that has been used to generate adaptive responses in nanotube systems^[8,36]. Buffers with a mixture of monovalent and divalent cations may enable isothermal assembly as well as stability in the presence of enzymatic reactions.

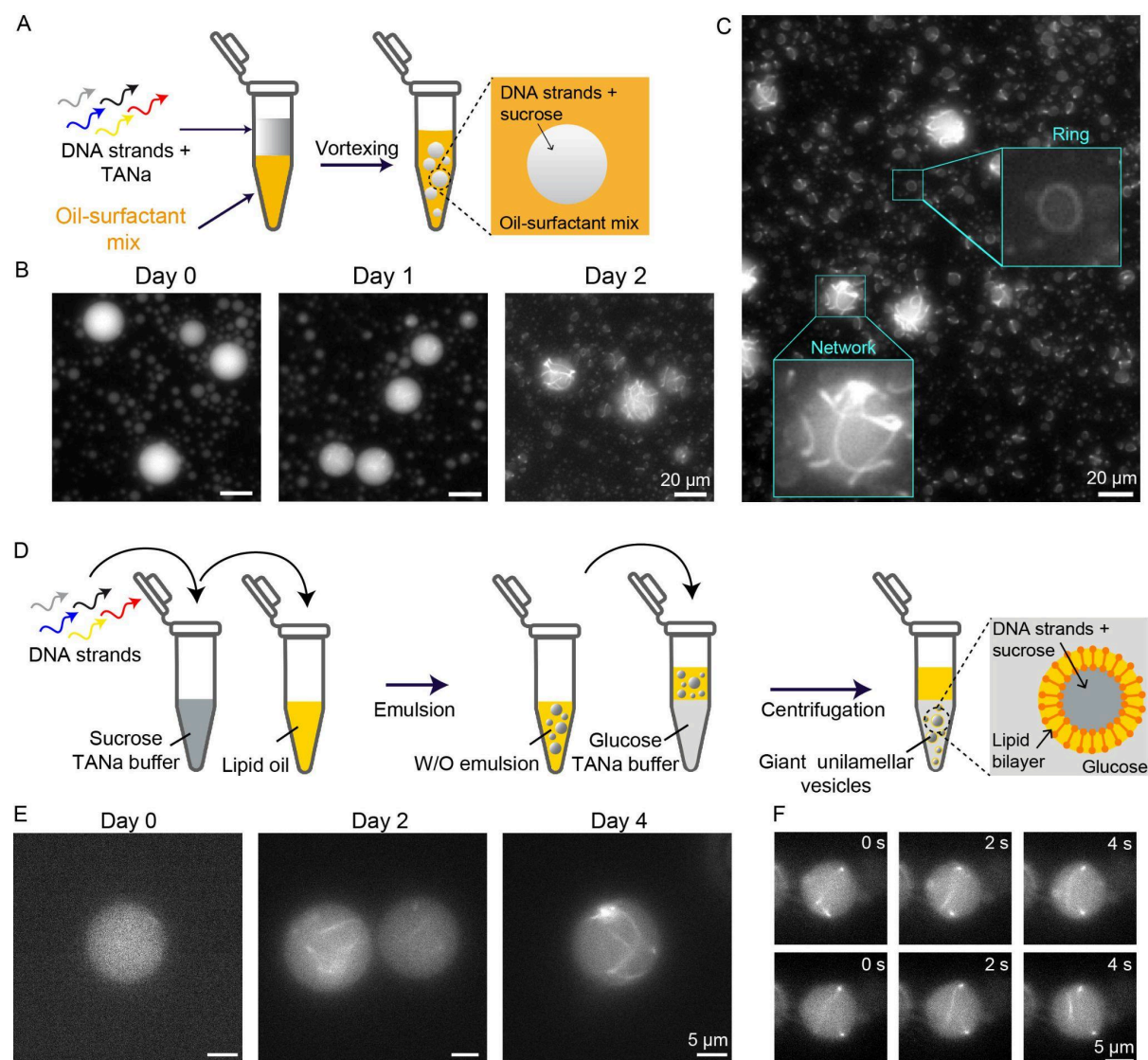


Figure 4: Isothermal growth and self-organization of DNA nanotubes in biomimetic confinement. A) Scheme showing the protocol for encapsulation of DNA strands inside water-in-oil droplets. B) Representative fluorescence microscopy images of nanotubes encapsulated in water-in-oil droplets in presence of TANA buffer at different time points (each strand concentration is 100 nM). C) Fluorescence microscopy image showing network and ring-like structure formation from the self-assembly of DNA strands inside droplets at room temperature. D) Scheme showing the protocol for encapsulation of DNA strands inside giant unilamellar vesicles (GUVs) using TANA buffer (100 mM NaCl) and glucose as the outer medium. Each GUVs contains the DNA strands and sucrose (to ensure iso-osmotic conditions) in the same buffer and is kept at room temperature. E) Representative fluorescence microscopy images of nanotubes growing and reorganizing inside the GUVs at different times after the DNA strands encapsulation. F) Time lapse fluorescence microscopy images of a representative GUV taken after 4 days of encapsulation, showing the dynamics of the formed networks. Each row is a different time lapse acquisition starting at $t = 0$.

The conditions used here to assemble DNA nanotubes also enable the isothermal assembly of more complex DNA structures including various types of DNA origami^[26]. For this reason, our work indicates that it may become possible to create DNA systems that take advantage of both origami methods^[37], known for achieving arbitrary nanometer scale patterning, as well as of tiling methods^[38], which easily produce micrometer scale assemblies. Strand- and tile-based assemblies also constitute convenient ingredients for algorithmic self-assembly,^[39] allowing to program higher-order morphologies through computation. The combination of all these traits may lead to the development of multiscale DNA materials rivaling the complexity and adaptability of biological assemblies. These materials may in turn be made responsive to strand displacement networks^[40] or to physical inputs^[18] to achieve an even greater level of adaptation.

Acknowledgements

E.F. acknowledges support by the DOE Office of Science (Office of Basic Energy Sciences) under award SC0010595, which paid for salary (E.F. and S.P.A.) and reagents. D.B. acknowledges funding received from the European Research council ERC under the European Union's "HORIZON EUROPE Research and Innovation Programme (Grant Agreement No 101096956)" and the Institut Universitaire de France IUF. L.B. acknowledges the Fondation de la Recherche Médicale FRM (ARF202209015925). We acknowledge the Cell and Tissue Imaging core facility (PICT IBI SA), Institut Curie, member of the French National Research Infrastructure France-BioImaging (ANR10-INBS-04).

References

- [1] H. Hess, J. L. Ross, *Chem. Soc. Rev.* **2017**, *46*, 5570–5587.
- [2] I. Gasic, T. J. Mitchison, *Curr. Opin. Cell Biol.* **2019**, *56*, 80–87.
- [3] G. M. Whitesides, B. Grzybowski, *Science* **2002**, *295*, 2418–2421.
- [4] N. C. Seeman, H. F. Sleiman, *Nat. Rev. Mater.* **2017**, *3*, 17068.
- [5] P. W. K. Rothemund, *Nature* **2006**, *440*, 297–302.
- [6] F. Hong, F. Zhang, Y. Liu, H. Yan, *Chem. Rev.* **2017**, *117*, 12584–12640.
- [7] P. W. K. Rothemund, A. Ekani-Nkodo, N. Papadakis, A. Kumar, D. K. Fygenson, E. Winfree, *J. Am. Chem. Soc.* **2004**, *126*, 16344–16352.
- [8] L. N. Green, H. K. K. Subramanian, V. Mardanlou, J. Kim, R. F. Hariadi, E. Franco, *Nat. Chem.* **2019**, *11*, 510–520.
- [9] S. Agarwal, M. A. Klocke, P. E. Pungchai, E. Franco, *Nat. Commun.* **2021**, *12*, 3557.
- [10] N. Arulkumaran, M. Singer, S. Howorka, J. R. Burns, *Nat. Commun.* **2023**, *14*, 1314.
- [11] M. Illig, K. Jahnke, L. P. Weise, M. Scheffold, U. Mersdorf, H. Drechsler, Y. Zhang, S. Diez, J. Kierfeld, K. Göpfrich, *Nat. Commun.* **2024**, *15*, 2307.
- [12] M. Glaser, J. Schnauß, T. Tschirner, B. U. S. Schmidt, M. Moebius-Winkler, J. A. Käs, D. M. Smith, *New J. Phys.* **2016**, *18*, 055001.
- [13] L. J. Stenke, B. Saccà, *Bioconjug. Chem.* **2023**, *34*, 37–50.
- [14] K. Jahnke, V. Huth, U. Mersdorf, N. Liu, K. Göpfrich, *ACS Nano* **2022**, *16*, 7233–7241.
- [15] B. Yurke, A. J. Turberfield, A. P. Mills Jr, F. C. Simmel, J. L. Neumann, *Nature* **2000**, *406*, 605–608.
- [16] K. Nakazawa, F. El Fakih, V. Jallet, C. Rossi-Gendron, M. Mariconti, L. Chocron, M. Hishida, K. Saito, M. Morel, S. Rudiuk, D. Baigl, *Angew. Chem. Int. Ed Engl.* **2021**, *60*, 15214–15219.
- [17] S. Agarwal, M. Dizani, D. Osmanovic, E. Franco, *Interface Focus* **2023**, *13*, 20230017.
- [18] A. Bergen, S. Rudiuk, M. Morel, T. Le Saux, H. Ihmels, D. Baigl, *Nano Lett.* **2016**, *16*, 773–780.
- [19] L. Zhou, P. Retailleau, M. Morel, S. Rudiuk, D. Baigl, *J. Am. Chem. Soc.* **2019**, *141*, 9321–9329.
- [20] S. M. Douglas, H. Dietz, T. Liedl, B. Högberg, F. Graf, W. M. Shih, *Nature* **2009**, *459*,

414–418.

- [21] H. Yan, S. H. Park, G. Finkelstein, J. H. Reif, T. H. LaBean, *Science* **2003**, *301*, 1882–1884.
- [22] S. Woo, P. W. K. Rothmund, *Nat. Commun.* **2014**, *5*, 4889.
- [23] Y. Suzuki, M. Endo, H. Sugiyama, *Nat. Commun.* **2015**, *6*, 8052.
- [24] G. Tikhomirov, P. Petersen, L. Qian, *Nature* **2017**, *552*, 67–71.
- [25] K. F. Wagenbauer, C. Sigl, H. Dietz, *Nature* **2017**, *552*, 78–83.
- [26] C. Rossi-Gendron, F. El Fakih, L. Bourdon, K. Nakazawa, J. Finkel, N. Triomphe, L. Chocron, M. Endo, H. Sugiyama, G. Bellot, M. Morel, S. Rudiuk, D. Baigl, *Nat. Nanotechnol.* **2023**, *18*, 1311–1318.
- [27] A. Ekani-Nkodo, A. Kumar, D. K. Fyngenson, *Phys. Rev. Lett.* **2004**, *93*, 268301.
- [28] V. Mardanlou, K. C. Yaghoubi, L. N. Green, H. K. K. Subramanian, R. F. Hariadi, J. Kim, E. Franco, *Nat. Comput.* **2018**, *17*, 183–199.
- [29] M. Pacella, V. Mardanlou, S. Agarwal, A. Patel, E. Jelezniakov, A. M. Mohammed, E. Franco, R. Schulman, *Systems Design & ...* **2020**, *5*, 544–558.
- [30] D. S. W. Lee, C.-H. Choi, D. W. Sanders, L. Beckers, J. A. Riback, C. P. Brangwynne, N. S. Wingreen, *Nat. Phys.* **2023**, *19*, 586–596.
- [31] M. Weitz, J. Kim, K. Kapsner, E. Winfree, E. Franco, F. C. Simmel, *Nat. Chem.* **2014**, *6*, 295–302.
- [32] A. Yamada, T. Yamanaka, T. Hamada, M. Hase, K. Yoshikawa, D. Baigl, *Langmuir* **2006**, *22*, 9824–9828.
- [33] L.-L. Pontani, J. van der Gucht, G. Salbreux, J. Heuvingh, J.-F. Joanny, C. Sykes, *Biophys. J.* **2009**, *96*, 192–198.
- [34] F. Ben Trad, V. Wieczny, J. Delacotte, M. Morel, M. Guille-Collignon, S. Arbault, F. Lemaître, N. Sojic, E. Labbé, O. Buriez, *Anal. Chem.* **2022**, *94*, 1686–1696.
- [35] X. Liu, Y. Zhao, P. Liu, L. Wang, J. Lin, C. Fan, *Angew. Chem. Int. Ed Engl.* **2019**, *58*, 8996–9011.
- [36] D. Sorrentino, S. Ranallo, F. Ricci, E. Franco, *Nat. Commun.* **2024**, *15*, 1–13.
- [37] S. Dey, C. Fan, K. V. Gothelf, J. Li, C. Lin, L. Liu, N. Liu, M. A. D. Nijenhuis, B. Saccà, F. C. Simmel, H. Yan, P. Zhan, *Nature Reviews Methods Primers* **2021**, *1*, 1–24.
- [38] A. Heuer-Jungemann, T. Liedl, *Trends Chem.* **2019**, *1*, 799–814.
- [39] D. Woods, D. Doty, C. Myhrvold, J. Hui, F. Zhou, P. Yin, E. Winfree, *Nature* **2019**, *567*, 366–372.
- [40] D. Y. Zhang, R. F. Hariadi, H. M. T. Choi, E. Winfree, *Nat. Commun.* **2013**, *4*, 1965.